Electronic Supplementary Material (ESI) for Nanoscale.

Supporting Information

Nanoconfinement effects of chemically reduced graphene oxide nanoribbons on poly(vinyl chloride)

Jun Ho Choe, Jisoo Jeon, Min Eui Lee, Jeong Jae Wie, Hyoung-Joon Jin, and Young Soo Yun**

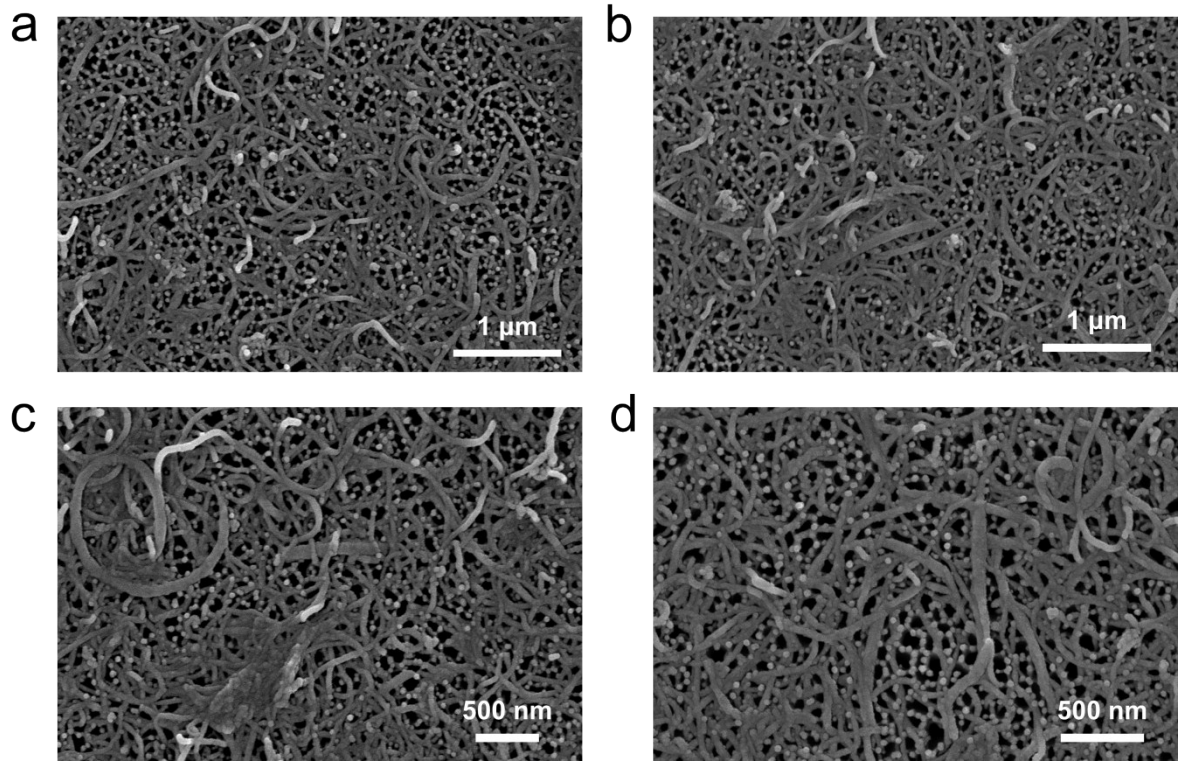

Figure S1. FE-SEM images of MWCNTs at various magnifications.

MWCNTs inherently contain numerous intrinsic defects in their graphene layer, such as heptagon–pentagon pairs, which can cause the tube to bend permanently.[1] These bent MWCNTs exhibit different characteristics than those of straight CNTs, and the bending ratio is an important parameter describing their specific characteristics. A quantitative factor for characterizing the various shapes of MWCNTs was therefore reported.[1–3] The bending ratio (D_b) is defined as the ratio of the mean-square end-to-end distance ($\langle R^2 \rangle$) to the square contour length (L^2)):

$$D_b \equiv \frac{\langle R^2 \rangle}{L^2} \tag{S1}$$

The relationship between the mesoscopic shape and the overall size is given by

$$\langle R^2 \rangle = 2l_{sp}L + 2l_{sp}^2\left(e^{-L/l_{sp}} - 1\right), \tag{S2}$$

where l_{sp} is the static bending persistence length and L is the contour length along the tube axis. For $L \gg l_{sp}$, or the "rigid random-coil limit," $\langle R^2 \rangle = 2l_{sp}L$. If $L < l_{sp}$, or the "rigid rod limit," then $\langle R^2 \rangle = L^2$. A large or small l_{sp} value indicates a large or small number of defects in the MWCNTs, respectively.

In our study, we used MWCNTs with high persistence length (l_{sp} ~520 nm) to prepare chemically unzipped MWCNTs, with high contour length and aspect ratio, as shown in Fig. S1.

[1] Lee HS, Yun CH, Kim HM, Lee CJ. Persistence length of multiwalled carbon nanotubes with static bending. J. Phys. Chem. C 2007; 111(51): 18882-18887.

[2] Lee HS, Yun CH, Kim SK, Choi JH, Lee CJ, Jin H-J, Lee H, Park SJ, Park M. Percolation of two-dimensional multiwalled carbon nanotube networks. Appl. Phys. Lett. 2009; 95(13): 134104.

[3] Yun YS, Kown HI, Bak H, Lee EJ, Yoon J-S, Jin H-J. Morphological Effects of Alkylated Multiwalled Carbon Nanotubes on Poly(L-lactic acid)-Based Composites. Macromol. Res. 2010; 18(9): 828-833.

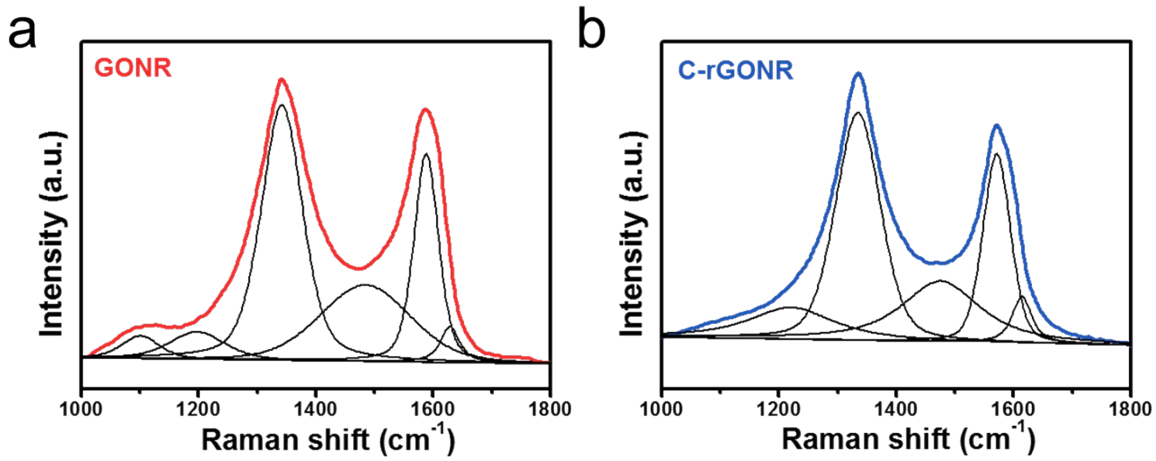

Figure S2. Deconvolved Raman spectra for (a) GONRs and (b) C-rGONRs.

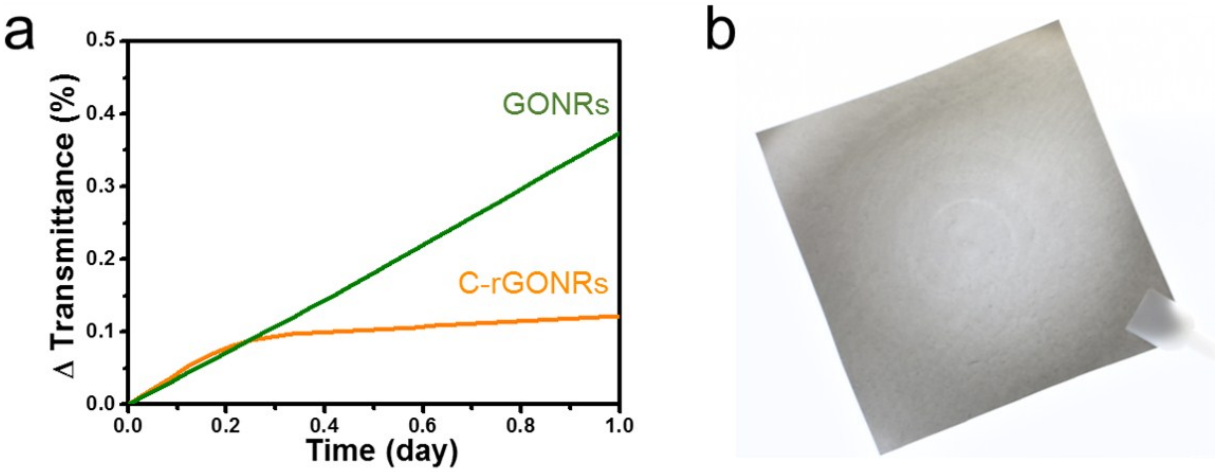

Figure S3. (a) Time vs. transmittance variation plot of GONRs and C-rGONRs dispersion in DMF obtained by Turbiscan. (b) Photographs of PVC films containing 0.1 wt% C-rGONR.

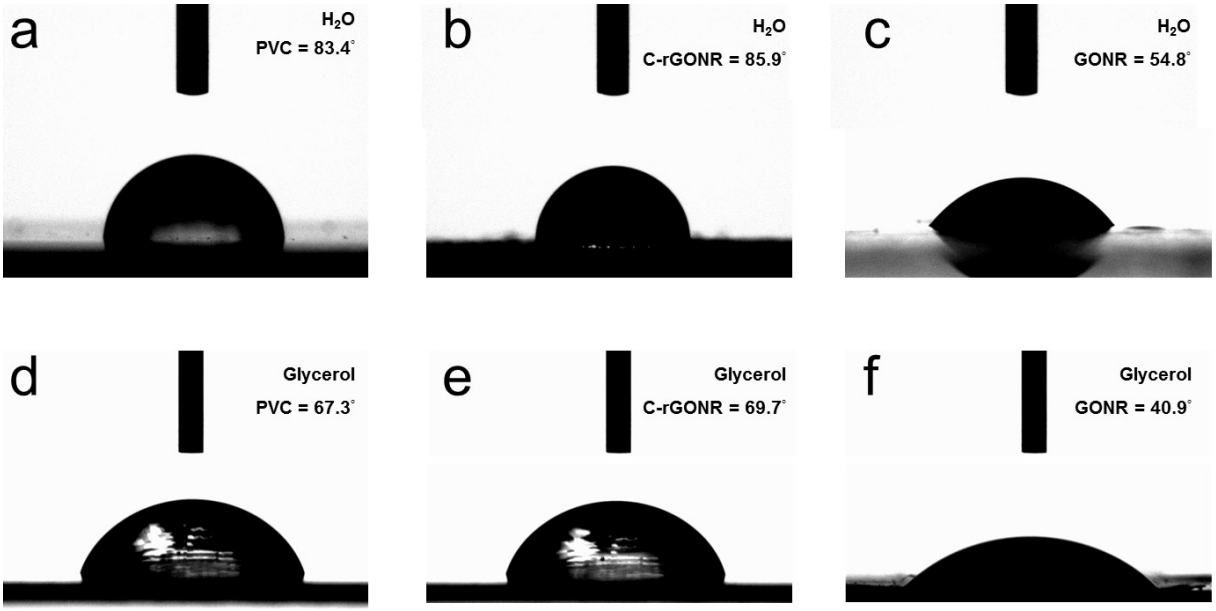

Figure S4. (a) Contact angle data of water on (a) PVC, (b) C-rGONRs and (c) GONRs films, and of glycerol on (d) PVC, (e) C-rGONRs and (f) GONRs films.

Table S1. Surface properties of PVC, C-rGONRs and GONRs.

	PVC	C-rGONR	GONR
Dispersion, γ^d [mJ/m^2]	29.3	28.9	27.8
Polarity, γ^p [mJ/m^2]	4.6	3.8	21.1
Surface energy, $\gamma = \gamma^d + \gamma^p$ [mJ/m^2]	33.9	32.7	48.9

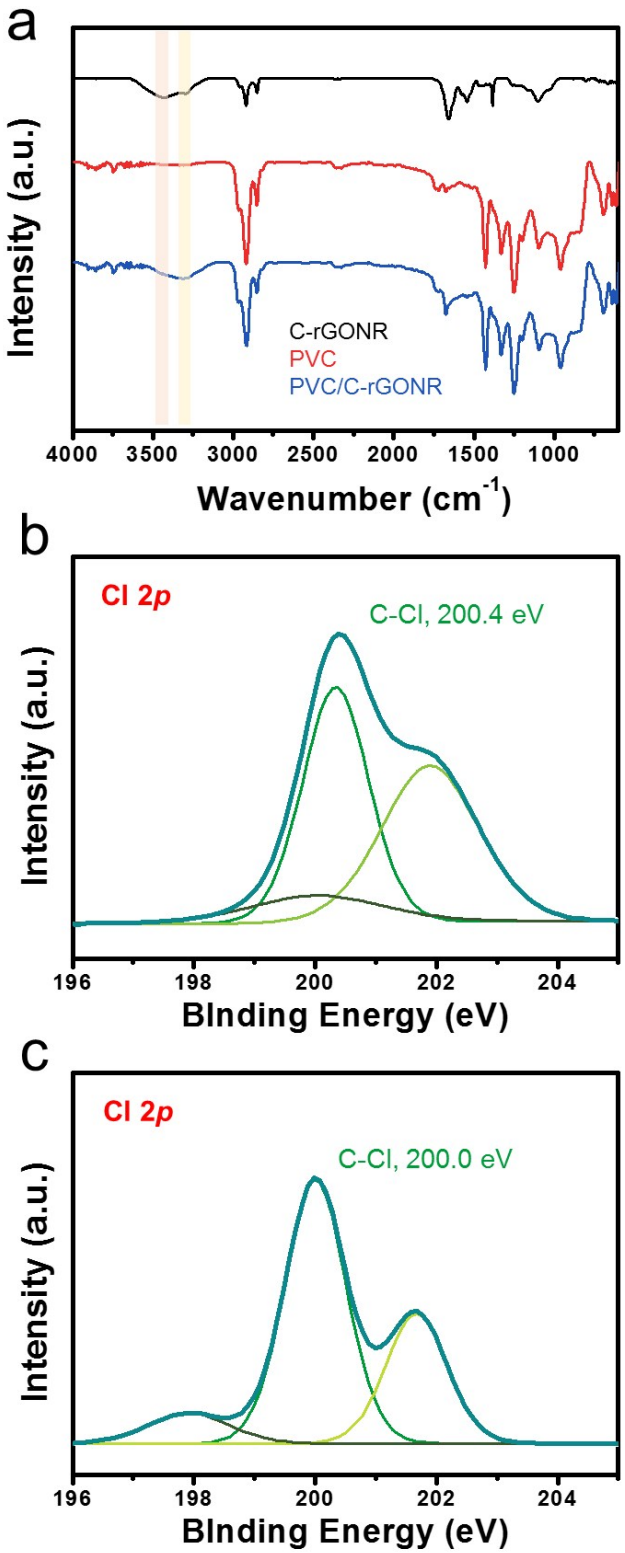

Figure S5. (a) IR spectra of C-rGONRs, PVC, and PVC/C-rGONRs, and XPS Cl 2*p* spectra of (b) PVC matrix and (c) PVC/C-rGONRs nanocomposite.